THE EFFECT OF PERIODIC BALLONET JET EXHAUST ON THE STABILITY OF A TETHERED AEROSTAT

S.M. Kannan*
National Aeronautical Laboratory
Bangalore 560 017. India

G.V. Rao**
Indian Institute of Science
Bangalore 560 012, India

Abstract

Tethered aerostats operating under wide range of altitudes and atmospheric pressure conditions employ ballonets within the hull filled with air. These ballonets exhaust the air into the atmosphere whenever necessary to maintain the difference between the atmospheric pressure and the internal pressure within a desired range. Assuming that the air exhaust is made periodic, studies are made *on* the effect of the periodic jet force and the resulting pitching moment *on* the response of the aerostat system. In the first phase, the stability of the system is studied by analysing the eigenvalues and eigenvectors. The result *shows* that the aerostat system is unstable in the windspeed range of 0-15 fps and stable in the windspeed range of 15-100 fps. When the system is subjected to a suitable periodic forcing from the exhaust jet, it is observed that it is not only possible to extend the stability boundary of 15 fps down to typically 5 fps, but much more interestingly, there exist forcing periods of the exhaust jet which render the system completely stationary.

Nomenclature

A	matrix of coefficients of the system dynamical eqs. (12)
B	total buoyant force of the aerostat
$\hat{C}$	damping coefficient defined in eq. 11
$dx_a/d\theta$	axial ballonet constraint term used in eq. 10
E	matrix of coefficients of the system dynamical eqs. (12)
FF	forcing function vector
g	gravitational acceleration
I_{yy}, I_{zz}	moments of inertia about the y and z axes, respectively
$\hat{K}$	spring constant defined by eq. 10
m	mass of the aerostat excluding the hull's Internal air and gas.
$\hat{M}$	equivalent mass term defined by eq. 9
m_a, m_g	masses of the hull's Internal air and gas, respectively.
$N_{\frac{1}{2}}$	number of cycles for unforced balloner slosh to damp to half amplitude
q	angular velocity about the y-axis
$\hat{Q}$	Complex eigenvector term for q from *eq.* 13
t	time
T	tether cable tension
$\hat{T}$	complex eigenvector term for δT from eq. 13
$\hat{U}$	complex eigenvector term for u from eq. 13
u	velocity of the mass centre of m in the x-direction
u_0	mean wind speed
v_a, v_g	mass-centre velocities of m_a and m_g respectively
V	Volume
$\hat{V}_a$	Complex eigenvector term for v_a from *eq.* 13
W_o	weight of the aerostat system
w	velocity of the mass centre of m in the z-direction
$\hat{W}$	complex eigenvector term for w from eq. 13
x , z	body-fixed wind axes originating at the mass centre of m
Y	body-fixed co-ordinate normal to x and z axes
X,Y,Z	forces on m in the x,y,z directions, respectively
$\hat{X}_a$	complex eigenvector term for δx_a from eq. 13

Greek symbols

α	aerodynamic angle of attack
γ	perturbed cable angle
Γ	cable angle defined in Fig. 1
$\hat{\Gamma}$	complex eigenvector term for γ from eq. 13
δ ( )	Quantity perturbed from equilibrium
η	real part of a
θ	aerostat pitch angle defined in Fig. 1
$\hat{\theta}$	complex eigenvector term for θ from eq. 13

* Scientist, Fluid Mechanics Division.

** Professor, Department of Aerospace Engg.

ρ density of the air at the aerostat altitude

σ stability root defined by eq. 13

ω imaginary part of σ

Subscripts

$( )_{tp}$ w.r.t. the tether-cable confluence point

$( )_a$ w.r.t the internal air of the hull

$( )_B$ w.r.t. the volume-tric centre of the aerostat's total displaced volume

$( )_c$ tether cable term

$( )_g$ w.r.t. the lifting gas in the hull

$( )_o$ reference equilibrium

$( )_q$ derivative of X,Z,M w.r.t. q

$( )_{\dot{q}}$ derivative of X,Z,M w.r.t. $\dot{q}$

$( )_u$ derivative of X,Z,M w.r.t. U

$( )_{\dot{u}}$ derivative of X,Z,M w.r.t $\dot{u}$

$( )_w$ derivative of X,Z,M w.r.t. w

$( )_{\dot{w}}$ derivative of X,Z,W w.r.t. $\dot{w}$

$( )_{\dot{\alpha}}$ derivative w.r.t. $\dot{\alpha}$

Superscript

$\dot{( )}$ derivative w.r.t. t

Introduction

A tethered aerostat (Fig.1) designed to operate over a wide range of altitudes and varying atmospheric pressure is usually provided with what is called a 'ballonet' (Fig.2). The ballonet is simply another flexible bag inside the hull, which is continuously filled with the atmospheric air by means of a blower. This flexible bag communicates pressure to the *gas* in the hull. The internal pressure is typically kept in the range of 5-20 cm of water column above the atmospheric pressure, In order to maintain the rigidity of the hull, without exceeding the allowable loadings on the hull structure, When the pressure exceeds the set higher limit, a pressure valve in the ballonet opens and discharges the excess air into the atmosphere. Since the blower is kept running all the time, the discharge valve operates intermittently so as to maintain the internal pressure within the higher limit. A theoretical investigation[1] was undertaken to *study* the effect of the impulsive periodic action of the exahust jet *on* the system response, together with the sloshing motions of the air mass in the ballonet described by DeLaurier[2]. The effec of variation of the cable tension along its lengt is not included in the present analyses.

Formulation of the Eigenvalue Problem

In the first phase of the *study,* the natural stability of the aerostat system is studied, without the action of the exhaust jet. The equations of motion of the system[2] are given by the following eight simultaneous first order linear differential equations:

$$X_u u + X_w w + X_q q + (B - W_o - T_o \sin\Gamma_o)\theta + \delta T \cos\Gamma_o - T_o \sin\Gamma_o \cdot \gamma - (-X_u + W_o/g)u - (-X_{\dot{w}} w) - (m_a z_{ao} + m_g z_{go} - X_{\dot{q}})\dot{q} - (m_a - m_g V_a/V_g)\dot{v}_a = 0 \quad (1)$$

(Force equilibrium equation in the x direction)

$$Z_u u + Z_w w + [Z_q + (W_o/g)U_o]\, q + T_o \cos\Gamma_o \theta + \sin\Gamma_o \cdot \delta T + T_o \cos\Gamma_o \cdot \gamma - (-Z_{\dot{u}})\dot{u} - (W_o/g - Z_{\dot{w}})\dot{w} - (m_a x_{ao} - m_g x_{go} - Z_{\dot{q}})\dot{q} = 0 \quad (2)$$

(Force equilibrium equation in the z-direction)

$$M_u u + M_w w + [M_q - (m_a x_{ao} + m_g x_{go})U_o]q + [Bz_B - (m_a z_{ao} + m_g z_{go})g - T_o (z_{tp} \sin\Gamma_o + x_{tp} \cos\Gamma_o)]\theta - (m_a - m_g V_a/V_g)\, g \cdot \delta x_a + (z_{tp} \cos\Gamma_o - x_{tp} \sin\Gamma_o)\delta T + [-T_o (z_{tp} \sin\Gamma_o + x_{tp} \cos\Gamma_o)]\gamma - [-M_{\dot{u}} + (m_a z_{ao} + m_g z_{go})]\dot{u} - [-M_{\dot{w}} - m_a x_{ao} - m_g x_{go}]\dot{w} - [I_{yy} + m_a (x_{ao}^2 + z_{ao}^2) + m_g (x_{go}^2 + z_{go}^2) - M_{\dot{q}}]\dot{q} - (m_a z_{ao} - m_g z_{go} V_a/V_g)\dot{v}_a = 0 \quad (3)$$

(pitching moment equilibrium equation)

$$v_a - \delta \dot{x}_a = 0 \quad (4)$$

$$q - \dot{\theta} = 0 \quad (5)$$

$$u + z_{tp}\dot{\theta} - (L \sin\Gamma_o) \cdot \gamma\} = 0 \quad (6)$$

$$w - U_o \cdot \theta - x_{tp}\dot{\theta} + L \cos\Gamma_o \cdot \dot{\gamma} = 0 \quad (7)$$

(equations (4) to (7) are kinematic relations).

$$(m_a - m_g V_a/V_g)g \cdot \theta + \hat{K}\delta x_a + (m_a - m_g V_a/V_g)\dot{u} + (m_a z_{ao} - m_g z_{go} V_a/V_g)\dot{q} + \hat{M}\dot{v}_a + \hat{C}\dot{\delta x_a} = 0 \quad (8)$$

(dynamic equation of the air and *gas* relative to the hull)

where,

$$\hat{M} = m_a + m_g (V_a/V_g)^2 \quad (9)$$

$$\hat{K} = (m_g V_a/V_g - m_a)\, g / (dx_a/d\theta) \quad (10)$$

$$\hat{C} = 0.2206 (\hat{K}\hat{M})^{\frac{1}{2}} / [(N_1)^2 - 0.01217]^{\frac{1}{2}} \quad (11)$$

The unknown quantities θ_o, T_o and Γ_o are determined from the longitudinal vertical and pitching moment equilibrium equations. The above

set of 8 simultaneous equations, may be represented in the following matrix notation:

$$[A] \begin{bmatrix} u \\ w \\ q \\ \theta \\ v_a \\ \\ \delta_T \\ \gamma \end{bmatrix} - [E] \begin{bmatrix} \dot{u} \\ \dot{w} \\ \dot{q} \\ \dot{\theta} \\ \dot{v}_a \\ \dot{\delta x_a} \\ \dot{\delta}_T \\ \dot{\gamma} \end{bmatrix} = 0 \quad \cdots\cdots\cdots\cdots (12)$$

where [A] and [E] are 8x8 matrices whose elements are the coefficients of the 8 equations. With the assumption of a harmonic solution,

$$[Y] = \begin{bmatrix} u \\ w \\ q \\ \theta \\ v_a \\ \delta x_a \\ \delta_T \\ \gamma \end{bmatrix} = \begin{bmatrix} \hat{U} \\ \hat{W} \\ \hat{Q} \\ \hat{\theta} \\ \hat{V}_a \\ \hat{X}_a \\ \hat{T} \\ \hat{\Gamma} \end{bmatrix} e^{\sigma t} \quad \cdots\cdots\cdots (13)$$

equation (12) leads to an eigenvalue problem.

From equations (12) and (13), we obtain

$$[[A] - \sigma [E]] [Y] = [0] \qquad (14)$$

$$\text{or, } [A] - \sigma [E] = 0 \qquad (15)$$

Pre-multiplying by A^{-1}, we get

$$[I - \sigma A^{-1} E] = [0]$$

Dividing throught by the scalar σ, we get

$$[A^{-1}E - I/\sigma] = [0] \qquad (16)$$

σ's are the reciprocals of the eigenvalues of $A^{-1}E$. The values thus obtained are plotted in Fig. 3. It is observed that the system is unstable below a windspeed of about 15 fps and stable in the speed range 15-100 fps.

System Response to Dynamical Inputs

The ballonet air exhaust jet is assumed to operate periodically in a square wave pattern. The range of forcing periods studied is 5-100 sec. The exhaust jet velocity is assumed to be 100 fps and the jet area 0.35 sq.ft. corresponding to 8 inch dia. outlet. The jet is assumed to act downwards normal to the body axis of symmetry at a distance of 11 ft. from the C.G. of the system. The jet reaction force and the resulting pitching moment are obtained from the relations:

$$FF(2) = -\rho A V_j^2 = -9 \text{ lb.}$$

$$FF(3) = -9 \times 11 \text{ ft.lb.} = -100 \text{ ft. lb.}$$

The forcing function vector thus becomes

$$FF = \begin{bmatrix} 0 \\ -9 \\ -100 \\ 0 \\ 0 \\ 0 \\ 0 \\ 0 \end{bmatrix} \quad \cdots\cdots\cdots\cdots\cdots (17)$$

The equations of motion (12) with the forcing inputs therefore take the final form:

$$[A] [Y] - [E] [\dot{Y}] + [FF] = [0] \qquad (18)$$

From these equations, the derivatives of the state variables are obtained as follows:

$$\dot{Y}_1 = [\Sigma A_{1j} Y_j - E_{13} \dot{Y}_3 - E_{15} \dot{Y}_5] / E_{11}$$

$$\dot{Y}_2 = [\Sigma A_{2j} Y_j - E_{23} \dot{Y}_3 + FF(2)] / E_{22}$$

$$\dot{Y}_3 = [\Sigma A_{3j} Y_j - E_{31} \dot{Y}_1 - E_{32} \dot{Y}_2 - E_{35} \dot{Y}_5 + FF(3)] / E_{33}$$

$$\dot{Y}_4 = Y_3$$

$$\dot{Y}_5 = [A_{84} Y_4 + A_{86} Y_6 - E_{81} \dot{Y}_1 - E_{83} \dot{Y}_3 - E_{86} \dot{Y}_6] / E_{85}$$

$$\dot{Y}_6 = Y_5$$

$$\dot{Y}_7 = 0$$

$$\dot{Y}_8 = [Y_1 - E_{64} \dot{Y}_4] / E_{68},$$

where Σ stands for summation over j = 1, 3

These are a system of 8 first order linear differential equations, which are solved using Runge-Kutta-Gill's numerical integration method.

Calculations of the response were made as follows: The initial perturbations were taken to be zero and the periodic operation of the jet exhaust assumed. Calculations were performed for one small value of the forcing amplitude and another at 10 times this value to see the effect of the amplitude of the forcing function. It was noticed that the amplitude of the various state variables started increasing in most cases, although the rate of increase depended on the forcing period. it was observed that corresponding to the large forcing amplitude, there were two forcing periods at all wind speeds at which, there was practically no build-up of the state variables with time. The results thus obtained are shown

in Figs. 4, 5 and 6. These calculations were made for two values of the amplitude of the forcing function.

Discussions of the Results

The most interesting observation from the above results is that there appears to be a specific period of the forcing function and its amplitude at all windspeeds at which the response parameters like perturbation velocities, pitch angle, pitch rate etc. remain practically zero. If the forcing amplitude is sufficiently large at a given windspeed, it appears to be possible to drive the system parameters to nearly zero magnitudes at small values of the forcing period, in addition to that at large forcing period. However, it seems relatively easy to drive the system amplitudes to nearly zero values at the second forcing period, which is larger than the first one. At the lowest windspeed of 10 fps, it is observed that the response amplitudes reach a minimum value at a forcing period of approximately 12 sec. This period is close to the natural short period mode of the aerostat (Fig. 4). As the wind speed is increased, two distinct forcing periods are observed (Figs. 5 and 6) at the higher amplitudes of the forcing function and the separation between these two periods increases with increasing windspeed. In fact, one could say that the two critical forcing periods nearly coincide at low windspeeds around 10 fps. However, if the amplitude of the forcing function is small, only one forcing period at which near-zero response amplitude is observed. The larger forcing period at which the system response is close to zero is a weak function of the amplitude of the forcing function. In Fig. 7, the forcing period for zero response has been plotted against wind speed for two amplitudes of the forcing function.

Also shown in Fig. 7 are the first and the third modes of oscillation of the system which correspond approximately with the inverted pendulum and the short period modes. One observes that while the inverted pendulum mode may have a bearing on the response amplitude of the system at lowspeeds, the critical forcing period for either suppressing or minimising the amplitude response lies somewhere in between the two natural periods.

Conclusions

The basic system is unstable in the wind speed range of 0-15 fps and stable in the wind speed range of 15-100 fps. When the system is subjected to a suitable periodic forcing from the exhaust jet, it is not only possible to extend the stability boundary of 15 fps down to 5 fps, but much more interestingly, there exist forcing periods of the exahust jet at which the system exhibits zero response. This indicates that a suitably tuned periodic jet exhaust can be employed as a dynamk vibration absorber and stabilise the system against all perturbation motions and render the tethered aerostat system practically stationary in the longitudinal mode. The limited studies reported In thls paper consider only the symmetric motion of the aerostat. It is well known that the lateral oscillations of the aerostat, particularly of the inverted pendulum mode, are perhaps of even greater importance. Any extension of the present approach for stabilising the aerostat in its lateral mode should assume that the discharge of the ballonet air should also be made in the lateral direction.

References

1. Kannan, S.M., "An Investigation of the Effect of the Ballonet Exhaust Jet on the Longitudinal Stability of a Kytoon", Project Dissertation submitted for the award of the degree of Master of Engineering at the Indian Institute of Science, Bangalore, 1980.

2. DeLaurier, James D., "An Investigation of the Effect of Ballonet Motions on Tethered Aerostat Longitudinal Dynamic Stability", UTIAS Technical Note No. 205, May 1977, University of Toronto, Institute for Aerospace Studies.

3. Rao, GNV, "Aerodynamic Stability of Tethered Bodies", Journal of Aircraft, Vol.14, March 1972, pp.315-317.

4. Etkin, B., "Dynamics of Flight", Wiley N.Y., 1959.

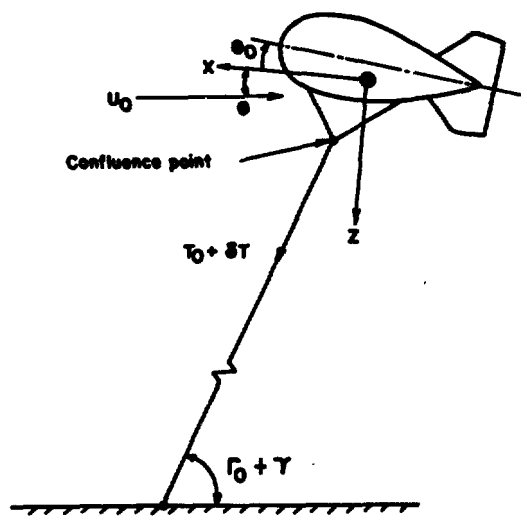

Fig.1 Coordinates for cable aerostat system

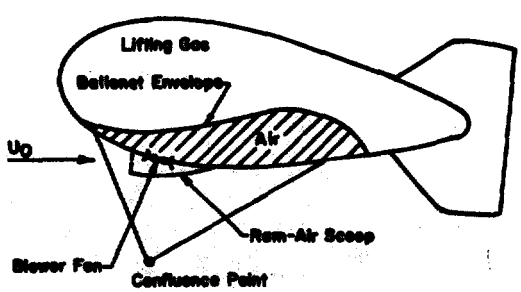

Fig.2 Schematic of typicol ballonet

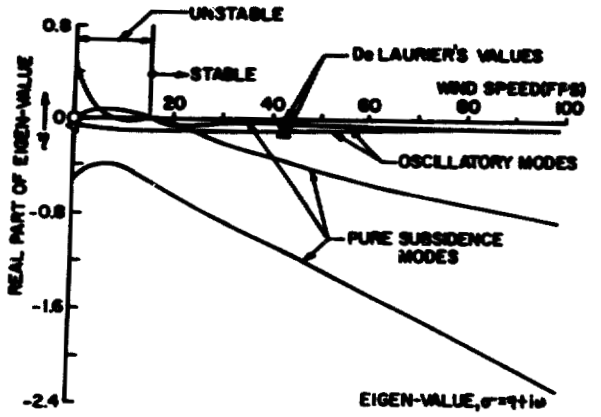

Fig.3 Variation of real part of stability roots with wind speed

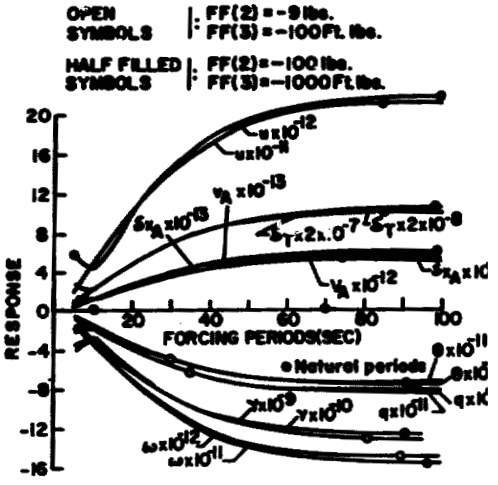

Fig.4 Response at 5 minutes at wind speed=10 fps. vs. forcing period

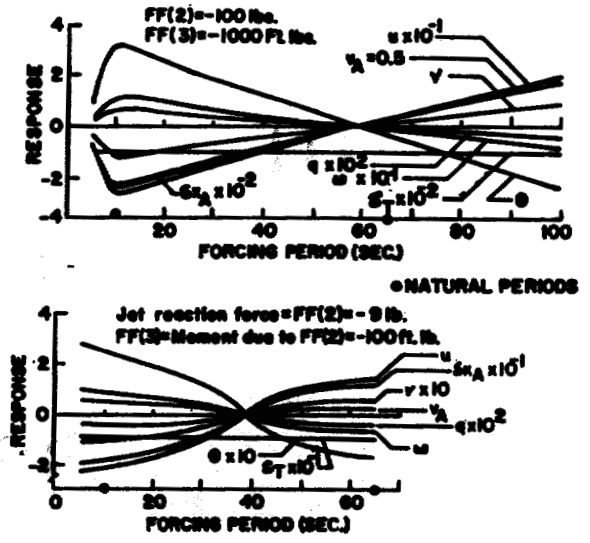

Fig.5 Response at 5 minutes at wind speed=42.2 fps. vs. forcing period

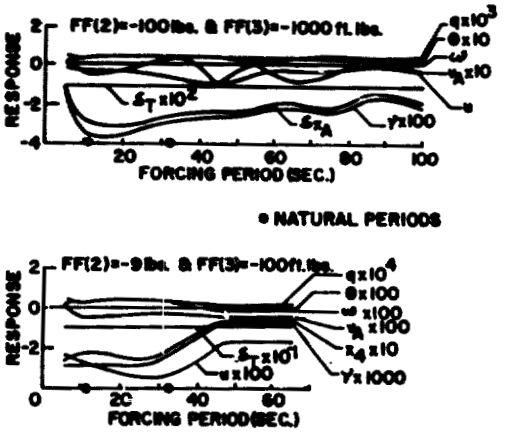

Fig.6 Response at 5 minutes at wind speed=100 fps. vs. forcing period

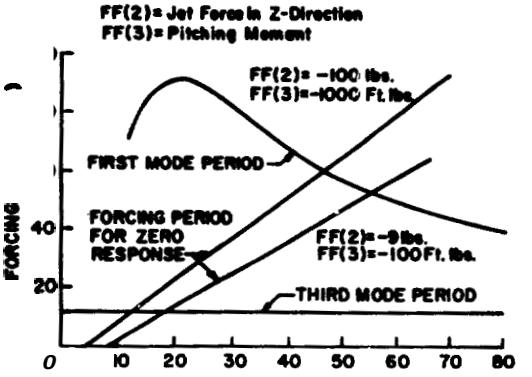

Fig.7 forcing period for zero response vs. windspeed

THE EFFECT OF PERIODIC BALLONET JET EXHAUST ON THE STABILITY OF A TETHERED AEROSTAT

S.M. Kannan*
National Aeronautical Laboratory
Bangalore 560 017. India

G.V. Rao**
Indian Institute of Science
Bangalore 560 012, India

Abstract

Tethered aerostats operating under wide range of altitudes and atmospheric pressure conditions employ ballonets within the hull filled with air. These ballonets exhaust the air into the atmosphere whenever necessary to maintain the difference between the atmospheric pressure and the internal pressure within a desired range. Assuming that the air exhaust is made periodic, studies are made on the effect of the periodic jet force and the resulting pitching moment on the response of the aerostat system. In the first phase, the stability of the system is studied by analysing the eigenvalues and eigenvectors. The result shows that the aerostat system is unstable in the windspeed range of 0-15 fps and stable in the windspeed range of 15-100 fps. When the system is subjected to a suitable periodic forcing from the exhaust jet, it is observed that it is not only possible to extend the stability boundary of 15 fps down to typically 5 fps, but much more interestingly, there exist forcing periods of the exhaust jet which render the system completely stationary.

Nomenclature

A	matrix of coefficients of the system dynamical eqs. (12)
B	total buoyant force of the aerostat
$\hat{C}$	damping coefficient defined in eq. 11
$dx_a/d\theta$	axial ballonet constraint term used in eq. 10
E	matrix of coefficients of the system dynamical eqs. (12)
FF	forcing function vector
g	gravitational acceleration
I_{yy}, I_{zz}	moments of inertia about the y and z axes, respectively
$\hat{K}$	spring constant defined by eq. 10
m	mass of the aerostat excluding the hull's Internal air and gas.
$\hat{M}$	equivalent mass term defined by eq. 9
m_a, m_g	masses of the hull's Internal air and gas, respectively.
$N_{\frac{1}{2}}$	number of cycles for unforced balloner slosh to damp to half amplitude
q	angular velocity about the y-axis
$\hat{Q}$	Complex eigenvector term for q from eq. 13
t	time
T	tether cable tension
$\hat{T}$	complex eigenvector term for δT from eq. 13
$\hat{U}$	complex eigenvector term for u from eq. 13
u	velocity of the mass centre of m in the x-direction
U_0	mean wind speed
v_a, v_g	mass-centre velocities of m_a and m_g respectively
V	Volume
$\hat{V}_a$	Complex eigenvector term for v_a from eq. 13
W_o	weight of the aerostat system
w	velocity of the mass centre of m in the z-direction
$\hat{W}$	complex eigenvector term for w from eq. 13
x, z	body-fixed wind axes originating at the mass centre of m
Y	body-fixed co-ordinate normal to x and z axes
X,Y,Z	forces on m in the x,y,z directions, respectively
$\hat{X}_a$	complex eigenvector term for δx_a from eq. 13

Greek symbols

α	aerodynamic angle of attack
γ	perturbed cable angle
Γ	cable angle defined in Fig. 1
$\hat{\Gamma}$	complex eigenvector term for γ from eq. 13
δ ( )	Quantity perturbed from equilibrium
η	real part of a
θ	aerostat pitch angle defined in Fig. 1
$\hat{\theta}$	complex eigenvector term for θ from eq. 13

* Scientist, Fluid Mechanics Division.
** Professor, Department of Aerospace Engg.